Journal of Cluster Science (2019) 30:131–139
https://doi.org/10.1007/s10876-018-1462-7

ORIGINAL PAPER

First-Principles Study of the Structures and Electronic Properties for Ni_nGe (n = 19–29) Clusters

Wei Song[1] · Zhe Fu[1] · Tian-hui Liu[4] · Jin-long Wang[1] · Bin Wang[1] · Wei Zhang[2] · Yuan Yuan[3]

Received: 27 October 2017 / Published online: 24 October 2018

Abstract

Using the density functional theory calculations with the PBE exchange–correlation energy functional, we have studied the magnetic property and electronic properties such as binding energy, embedding energy, charge transfer, ionization potential and electron affinity of the Ni_nGe (n = 19–29) neutral and ionic clusters. The addition of Ge atom can decrease the magnetic moments of Ni_n clusters except Ni_{28} and $Ni_{28}^{+/-}$. The charge is transferred from Ge atom to Ni clusters. And the local maxima value has appeared at $Ni_{25}Ge$ cluster. Both the calculated ionization potential and electron affinity exhibit an oscillating behavior as the cluster size increases.

Keywords First-principle · Magnetic property · Charge transfer · Ionization potential · Electron affinity

Introduction

The study of the electronic structure and properties of atomic clusters is an extremely active area of research due to its importance in nanoscience and nanotechnology. In the past three decades, considerable theoretical and experimental effort has been devoted to the understanding of pure transition metal clusters. However, in recent years, more and more attention has been paid to the study of the physical and chemical properties of bimetallic clusters. Because the bimetallic clusters have potential application in many fields such as catalyst, corrosion, heat resistance, magnetism and so forth. Ni clusters have been widespread concerned in catalytic reaction and magnetic materials because of their unique geometrical structures and delocalized d electrons. Therefore the bimetallic systems of many metals such as Ge [1, 2], Al [3], Fe [4], Rh [5], Pd [6], Ti [7], Cu [8], Mn [9] or others adsorbed Ni clusters have been reported. It is well known that Ge plays an important role in the development of the semiconductor industry. So Ni-Ge clusters are the primary target because of their wide applications in advanced material technology. Unfortunately, as regards Ni-Ge clusters, to the best of our knowledge, only a few studies have reported. To give some examples, Feng et al. studied ab initio calculations of the structures, binding energy and total spin moment of Ni_nGe (n = 2–12) clusters using all electron density-functional method. Their results showed that the doped Ge made both stability and magnetism of Ni_nGe clusters weakened as compared with pure Ni_{n+1} clusters [1]. Dhaka et al. [2] calculated the geometry, electronic structures, growth behavior and stability of neutral and ionized Ni encapsulated Ge clusters within the framework of a linear combination of atomic orbital density functional theory (DFT) under a spin polarized generalized gradient approximation. Moreover there are several studies which have been performed to analyze the structure, electronic and magnetic properties of transition metal impurities in Ge clusters [10, 11]. Thus the study of Ge on the configurations and electronic properties of Ni clusters has very important

✉ Wei Zhang
zhangw_bxx@jlu.edu.cn

✉ Yuan Yuan
16561458@qq.com

1 Physics and Electronic Engineering Department, Xinxiang University, Xinxiang 453003, People's Republic of China

2 Institute of Theoretical Chemistry, Jilin University, Changchun 130012, Jilin, People's Republic of China

3 School of Basic Science, Changchun University of Technology, Changchun 130012, People's Republic of China

4 Electronic Information Products Supervision Inspection Institute of Jilin Province, Changchun 130022, People's Republic of China

significance. Such clusters enhance stability because the semiconductor atom absorbs the dangling bonds present on the transition metal cages. Simultaneously, the cluster exhibits a wide range of electronic properties by varying the doping elements. If clusters are to be used for synthesizing materials, one must understand how sensitive their tailored properties are to size and topology. Unfortunately, there are very few experimental techniques can determine cluster structure, which is mainly because nanoclusters are too small to be detected using diffraction techniques and too large to be explored using spectroscopy. Therefore, theoretical calculations are particularly important. Usually the properties of clusters are sensitive to the size and the constituent element types for clusters, so the study of structures and properties for clusters on the one hand can help us to understand some of the features and laws condensed matter, and on the other hand play a guiding role in experimental synthesis.

The purpose of the present work is to perform the equilibrium structures of the Ni_nGe (n = 19–29) clusters theoretically by applying the DFT method implemented in the VASP code with the spin polarized PBE (Perdew, Burke, and Ernzerhof) gradient-corrected exchange–correlation functional method. Based on the neutral and ionic Ni_nGe clusters structures optimized from our DFT-PBE calculations, the magnetic moment, binding energy, embedding energy, charge transfer, adiabatic ionization potential and adiabatic electron affinity of the clusters as the cluster size increases have been systematically analyzed, which can provide useful information for the stability and electronic properties of Ni-Ge clusters in this range. The purpose of this study is to provide the fundamental data for the future estimation of the magnetic alloy materials.

Small size range Ni-Ge alloy clusters have been studied the theoretically before [12–14], but due to the smaller size range study can not provide clear growth behavior, structural and electronic properties of the series. Therefore, a study of the range is important from a realistic point of view and would be helpful to compare with the experimentally obtained data over a wide size range in future. The main focus of the present study is to explain the thermodynamic stability of clusters in neutral and charged states along with their chemical properties in detail.

Computational Methods

In the present theoretical work, we have verified the lowest-energy structures of neutral and ionic Ni_n (n = 19–29) clusters derived from Refs. [15–18] using density functional theory (DFT) calculations firstly. Next according to the lowest-energy structures of Ni clusters, the stable structures of neutral and ionic Ni_nGe (n = 19–29) clusters have been obtained. DFT has evolved into a widely applicable computational technique, while requiring less computational effort than convergent quantum mechanical methods such as coupled cluster theory. And our calculations are carried out using VASP code [19, 20] with the Perdew, Burke, and Ernzerhof (PBE) gradient-corrected exchange–correlation energy functional. The cutoff energy of plane wave (PW) in the calculations is taken to be 269.5 eV. A simple cubic supercell of size of 20 Å is used. The geometry optimization of each isomer was carried out till the energy is converged to an accuracy of 10^{-5} eV.

In order to understand the relative stability of the Ni_nGe (n = 19–29) clusters, we have analyzed the binding energy (BE) for neutral and ionic Ni_nGe compared to Ni_n clusters. BE is defined as the energy gained in assembling a cluster from its isolated constituents. The BE of Ni_n and Ni_nGe clusters are calculated according to the following definition [21–27],

$$BE(Ni_n) = [nE_{total}(Ni) - E_{total}(Ni_n)]/n$$
$$BE(Ni_nGe) = [nE_{total}(Ni) + E_{total}(Ge) - E_{total}(Ni_nGe)]/n + 1$$

where E_{total} (Ni_n) and E_{total} (Ni_nGe) are the total energy of Ni_n and Ni_nGe clusters. $E_{total}(Ni)$ and $E_{total}(Ge)$ are the energy of a free Ni and Ge atom, respectively.

Next, we also define the BE of Ni_n and Ni_nGe ionic clusters

$$BE\left(Ni_n^{+/-}\right) = \left[(n-1)E_{total}(Ni) + E_{total}\left(Ni^{+/-}\right) - E_{total}\left(Ni_n^{+/-}\right)\right]/n$$
$$BE\left(Ni_nGe^{+/-}\right) = \left[nE_{total}(Ni) + E_{total}\left(Ge^{+/-}\right) - E_{total}\left(Ni_nGe^{+/-}\right)\right]/n + 1$$

in which E_{total} ($Ni_n^{+/-}$) and E_{total} ($Ni_nGe^{+/-}$) are the total energy of the $Ni_n^{+/-}$ and $Ni_nGe^{+/-}$ clusters, $E_{total}(Ni^{+/-})$ and E_{total} ($Ge^{+/-}$) are the energy of a free $Ni^{+/-}$ and $Ge^{+/-}$ ion.

In addition, we have calculated the embedding energy (EE), which is the energy gain in incorporating a Ge atom in the lowest energy isomer of the pure Ni_n cluster [21–27]. In the case of Ni_nGe clusters, this is defined as

$$EE = E_{total}(Ni_n) + E_{total}(Ge) - E_{total}(Ni_nGe)$$

The configurations of Ni and Ge atoms are $3d^84s^2$ and $4s^24p^2$, respectively. We set the spin in our calculation process, and the total spin value is one, so the spin multiplicity of the ground state structures for Ni_nGe clusters are three, which follow the Wigner-Witmer (WW) spin conservation [21–27].

For charged clusters, there are two possibilities,

$$EE = E_{total}\left(Ni_n^{+/-}\right) + E_{total}(Ge) - E_{total}(Ni_nGe)$$

or

$$EE = E_{total}(Ni_n) + E_{total}\left(Ge^{+/-}\right) - E_{total}(Ni_nGe)$$

either the charged Ge atom can be embedded in a neutral Ni_n cluster or the other way round. We take the lower of these two numbers as the EE with enforcement of the WW spin conservation rule.

Results and Discussion

Structures of the Neutral and Ionic Ni_nGe (n = 19–29) Alloy Clusters

In this section, we have discussed the structures of Ni_nGe (n = 19–29) clusters. And a number of isomers are calculated at each size. Only selected isomers with energy close to the supposed ground state structures are presented in Fig. 1. It has been shown by previous experimental and theoretical studies that the lowest-energy structure of Ni_{19} is a perfect double-interpenetrating icosahedron, which has three parallel pentagonal rings stacked in a 1-5-1-5-1-5-1 sequence. The ground-state structures, the first and the second adsorption structures (wherever applicable) are marked (a), (b) and (c), respectively. The structures and relative energies presented in this work are all resulted from the DFT-PBE calculations. The lowest-energy structure of $Ni_{19}Ge$ can be viewed as adding one Ge atom to the cluster side face in the waist of Ni_{19}. And the Ni-Ge average bond length is calculated to be 2.365 Å, which is shortened compared to the optimized Ni_{19} clusters (2.484 Å). The other two low-energy adsorption structures ($Ni_{19}Geb$ and $Ni_{19}Gec$) are lying 0.409 and 0.682 eV higher above $Ni_{19}Gea$. The $Ni_{20}Gea$ is formed by adding one Ni atom and Ge atom on the adjacent waist sites of Ni_{19}, which is similar to the lowest-energy structure of Ni_{21} [17]. Next, in a similar fashion, the $Ni_{21}Gea$ is obtained by adding one Ge atom above the adjacent centre of equilateral triangle in the Ni_{21}. The Ni-Ge average bond lengths of $Ni_{20}Gea$ and $Ni_{21}Gea$ are 2.389 and 2.372 Å, which are shorter than the optimized Ni_{20} and Ni_{21} clusters (2.416 and 2.434 Å). It is found to be 0.054 and 0.430 eV ($Ni_{20}Geb$ and $Ni_{20}Gec$), 0.029 and 0.147 eV ($Ni_{21}Geb$ and $Ni_{21}Gec$) higher in energy than $Ni_{20}Gea$ and $Ni_{21}Gea$, respectively. The Ni_{23} can be seen as three interpenetrating 13-atom icosahedrons. The $Ni_{22}Gea$ is viewed as substitution of one Ni atom above centre of equilateral triangle by one Ge atom of Ni_{23} [17]. And the average bond lengths of the Ni-Ge (2.511 Å) for $Ni_{22}Gea$ can increase compared to the Ni–Ni (2.431 Å) for Ni_{22}. The low-energy adsorbed structures $Ni_{22}Geb$ and $Ni_{22}Gec$, 0.029 and 0.135 eV less stable than $Ni_{22}Gea$. The $Ni_{23}Gea$ and $Ni_{24}Gea$ are found to be one Ge atom located at the adjacent centre of equilateral triangle. The lowest-energy structures of Ni_{26} and Ni_{29} are considered to be composed of two interpenetrating 19-atom double-icosahedrons, and two interpenetrating double-icosahedrons and double-icositetrahedrons (with three parallel hexagonal rings), respectively [17]. And the average bond lengths are shortened from 2.471 to 2.443 Å for Ni–Ni (Ni_{23} and Ni_{24}) to 2.379 and 2.389 Å for Ni-Ge ($Ni_{23}Gea$ and $Ni_{24}Gea$). The energies of adsorption structures ($Ni_{23}Geb$ and $Ni_{23}Gec$, $Ni_{24}Geb$ and $Ni_{24}Gec$) are more than 0.172 and 0.476 eV, 0.071 and 0.205 eV above $Ni_{23}Gea$ and $Ni_{24}Gea$. The energetically most favorable structure of $Ni_{25}Gea$ from our present study can be viewed as substitution of one Ni atom by one Ge atom to the waist site of Ni_{26}. The average bond lengths of the Ni-Ge (2.571 Å) for $Ni_{25}Gea$ can increase compared to the Ni–Ni (2.491 Å) for Ni_{25}. And the $Ni_{25}Geb$ and $Ni_{25}Gec$ are 0.148 and 0.334 eV higher in energy than $Ni_{25}Gea$, respectively. The structures of $Ni_{26}Gea$ and $Ni_{29}Gea$ are viewed as adding one Ge atom at an adjacent hollow rhombus site in the waist of double-icosahedral structures for Ni_{26} and Ni_{29}. The $Ni_{27}Gea$ can be viewed as adding one Ni atom to the cluster side face in the waist of $Ni_{26}Gea$. We can remove one Ni atom on the top site of pentagonal pyramid of $Ni_{29}Gea$ to form the $Ni_{28}Gea$. The average bond lengths of Ni-Ge for $Ni_{26}Gea$, $Ni_{27}Gea$, $Ni_{28}Gea$ and $Ni_{29}Gea$ are 2.384, 2.386, 2.577 and 2.375 Å. The average bond length of Ni-Ge is increasing and decreasing for $Ni_{28}Gea$ and $Ni_{26,27,29}Gea$, respectively. The relative energies of the $Ni_{26}Geb$, $Ni_{27}Geb$($Ni_{27}Gec$) $Ni_{28}Geb$($Ni_{28}Gec$) and $Ni_{29}Geb$($Ni_{29}Gec$) are 0.438, 0.074(0.115), 0.071(0.281) and 0.108(0.478) eV higher compared to $Ni_{26}Gea$, $Ni_{27}Gea$, $Ni_{28}Gea$ and $Ni_{29}Gea$, respectively. Because of the high symmetry, there is only one kind of adsorption isomer for Ni_{26} cluster. It has been found that the lowest-energy structures of the cluster ions are almost identical with the neutral ones.

Relative Stabilities

The calculated Binding energies (BEs) for neutral and ionic Ni_nGe compared to Ni_n clusters are shown in Fig. 2a–c. It is found from observing Fig. 2a–c that the BEs of neutral and ionic Ni_nGe clusters is higher than the corresponding Ni_n clusters, showing that Ni-Ge alloy clusters are relatively more stable. This is mainly because Ge is a relatively stable semiconductor material. When the Ge atom is adsorbed to the active transition-metal Ni_n clusters, the stability of Ni_nGe clusters is relatively enhanced. The curve of BEs is seen to increase monotonically as a function of cluster size, which shows that the cluster can continue to gain energy during the growth process, and the adsorption of Ge atom is beneficial to improve the stability of the cluster. We also find that the BEs of cationic clusters

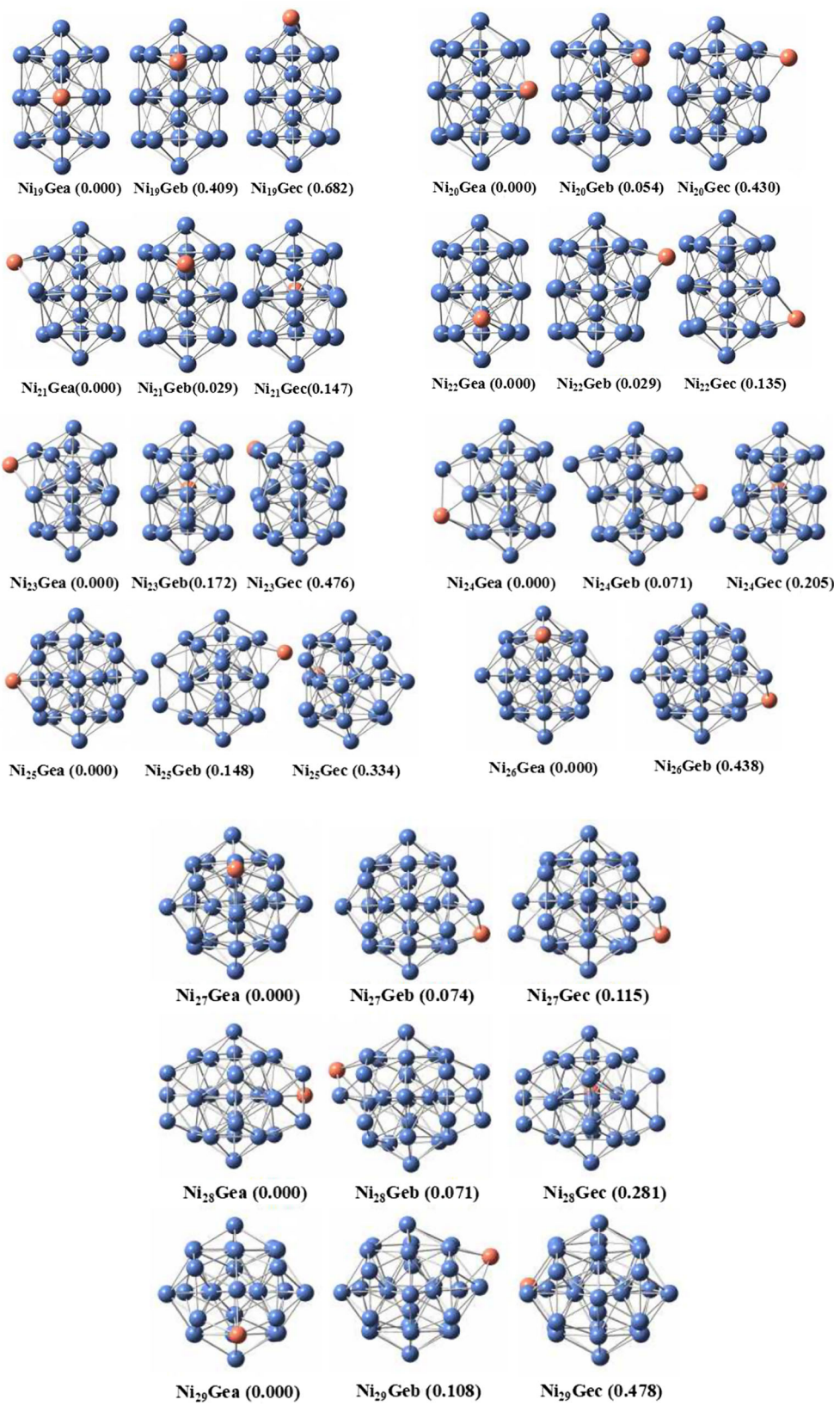

Fig. 1 Low-energy adsorption structures of the Ni_nGea (n = 19–29) clusters and relative energies (in eV) calculated at the DFT-PBE level

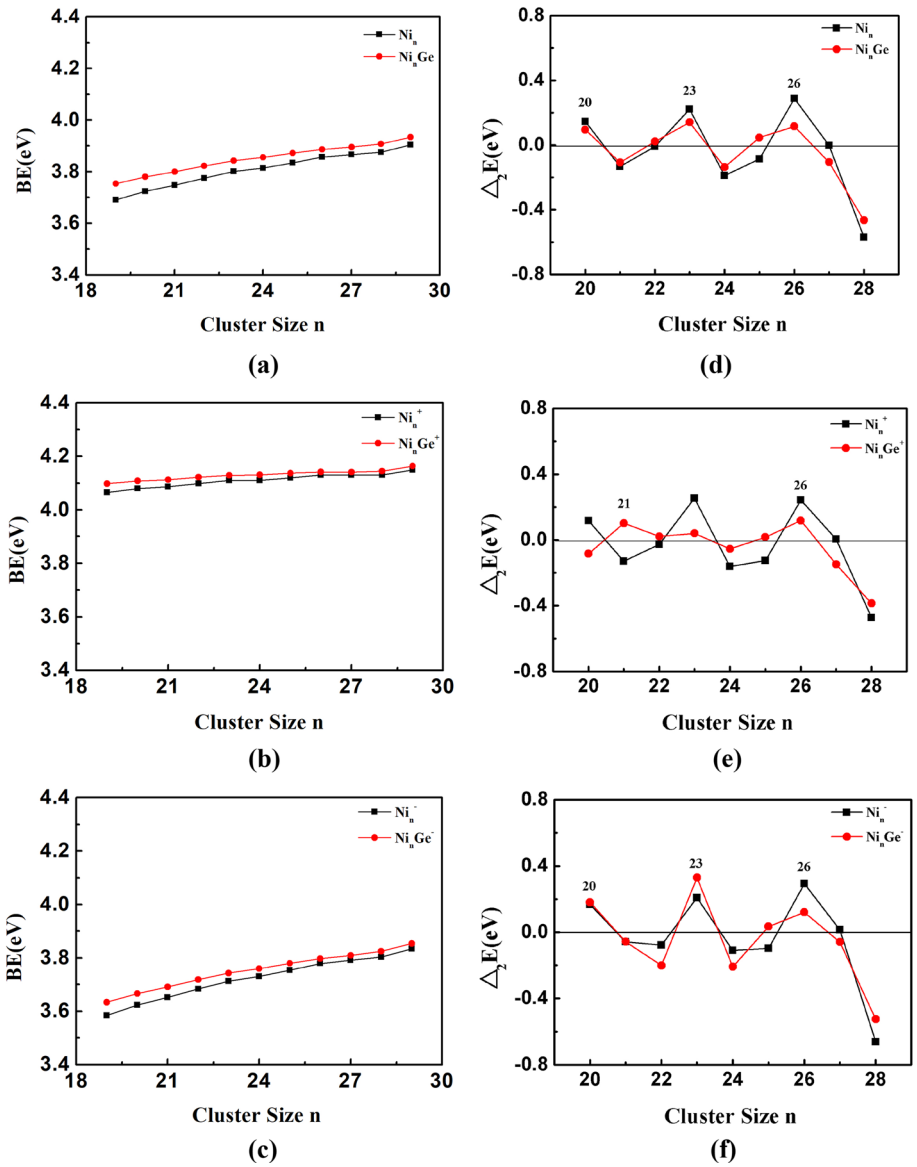

Fig. 2 Binding energy (BE) of Ni_n and Ni_nGea (n = 19–29) for **a** neutral, **b** cationic, and **c** anionic clusters; and second difference in energy of Ni_n and Ni_nGea (n = 20–28), for **d** neutral, **e** cationic, and **f** anionic clusters

are significantly higher than of neutral clusters, whereas anionic clusters are just the opposite. It can be seen from that the neutral clusters transit to an ionic clusters, the stability of the cluster structures change to some extent due to the change in the number of electrons.

The relative stability of the clusters can be also estimated through the second difference in energy which is defined by $\Delta_2E(n) = E(n+1) + E(n-1) - 2E(n)$ in which E(n) represents the total energy of cluster of size n. According to this definition, the clusters with positive Δ_2E are more stable than those with negative Δ_2E. The second difference in energy is a sensitive quantity that can reflect the relative stability of clusters and can be directly compared with the experimental relative abundance. The calculated Δ_2E for the Ni_n and Ni_nGea clusters are plotted in Fig. 2d, showing an oscillating behavior. Ni_nGea at n = 20, 23 and 26 correspond to the local maxima on the curve of Δ_2E, indicating that they are relatively more stable than the

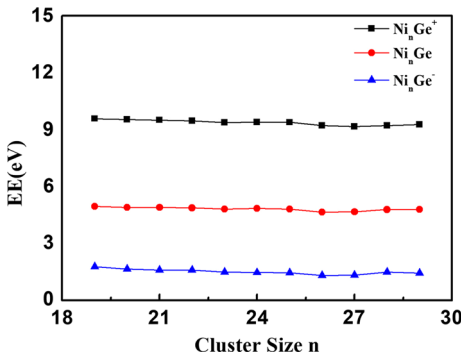

Fig. 3 Embedding energy (EE) of neutral and ionized Ni_nGea (n = 19–29) clusters

others. For the ionic clusters, there are several peaks on Δ_2E curve at n = 21 and 26 for the cationic clusters, and at n = 20, 23 and 26 for the anionic clusters, showing these cluster ions are relatively more stable in Fig. 2e, f.

Figure 3 shows the embedding energies (EEs) of Ni_nGea neutral, cationic and anionic clusters as a function of cluster size n. It is clear that there is not significant change in the EEs with the increase in cluster size. Similar to the BEs, the EEs of neutral clusters have lower and higher than cationic and anionic clusters, respectively.

Magnetic Properties

Ni clusters are typically ferromagnetic transition-metal clusters in the 3d group. The configuration of the Ni atom is $3d^84s^2$. The spin of the electron follows the Pauli exclusion principle and the Hund's rules, and the two unpaired 3d electrons of the Ni atom will contribute to its magnetic property. In principle, both spin and orbital magnetic moments have contribution to the total magnetic moment in any system. The orbital magnetic moment can be produced by orbital motion of each electron while the spin magnetic moment can be produced by electron spin. For ferromagnetic transition metal clusters, the magnetic moment mainly comes from the spin motion of the electron, while the orbital magnetic moment has almost no contribution to the total magnetic moment, which is called "orbital quenching effect". This conclusion has also been proven by recent experiments [25, 28]. Therefore, for the transition metals in the 3d group, the magnetic moment which is caused by the unpaired electron orbital motion is relatively small. The atomic total magnetic moment depends mainly on the electronic spin magnetic moment. As shown in Fig. 4a, the total magnetic moments obtained for Ni_nGea clusters from our calculation have the same trend as pure Ni_n clusters, which increase monotonically as a function of cluster size except $Ni_{28}Gea$. The calculated total magnetic moments decrease with the addition of Ge atom, but the Ge atom in all these clusters has negligible magnetic moments, which is in good agreement with previous results [19]. This is mainly due to a strong hybridization between the $3d^8$ of Ni with the $4s^24p^2$ of Ge atom results in the magnetic moment of Ni being quenched with leftover part to hold its spin moment in the Ni_nGe ground state cluster. The present investigation follows the same reported [25] and is one of the strongest evidence of the quenching of spin magnetic moment of the Ni atom. However the total magnetic moment of $Ni_{28}Gea$ is higher than Ni_{29}. In order to analyze the reasons for this phenomenon, we have plotted the total density of states (TDOS) for Ni_{28} and $Ni_{28}Gea$ clusters in Fig. 5a, b and the projected density of states (PDOS) for $Ni_{28}Gea$ in Fig. 5c, d. It can be seen from Fig. 5a, b, the structure of $Ni_{28}Gea$ can be considered to be composed of two interpenetrating

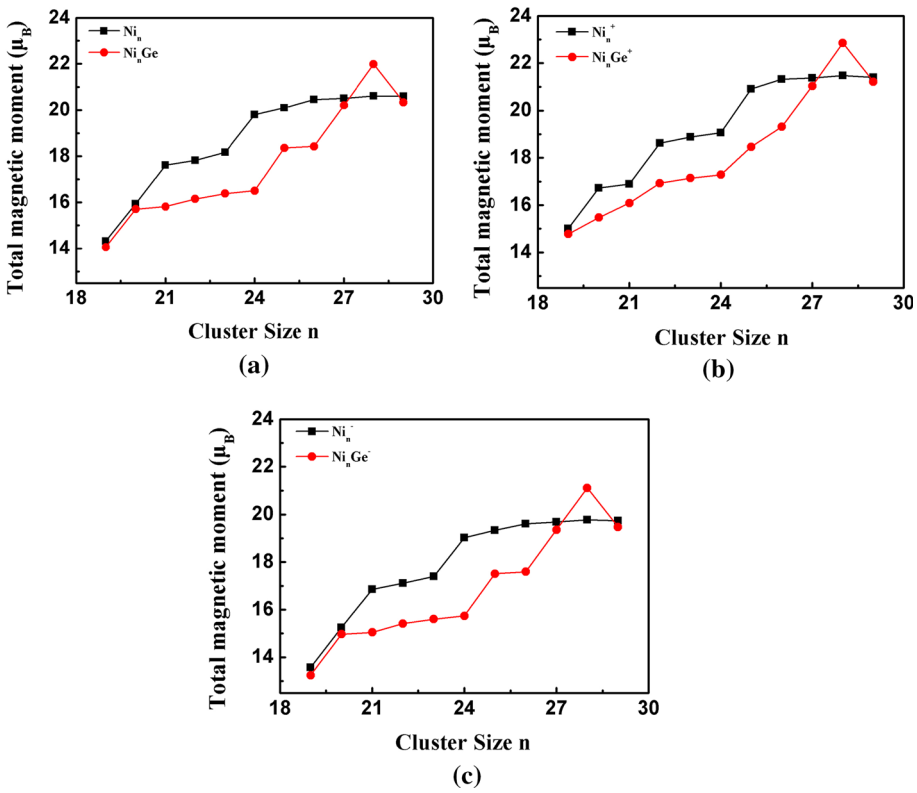

Fig. 4 The total magnetic moment (in units of μ_B) of Ni_n and Ni_nGea (n = 19–29) clusters for **a** neutral, **b** cationic, and **c** anionic clusters

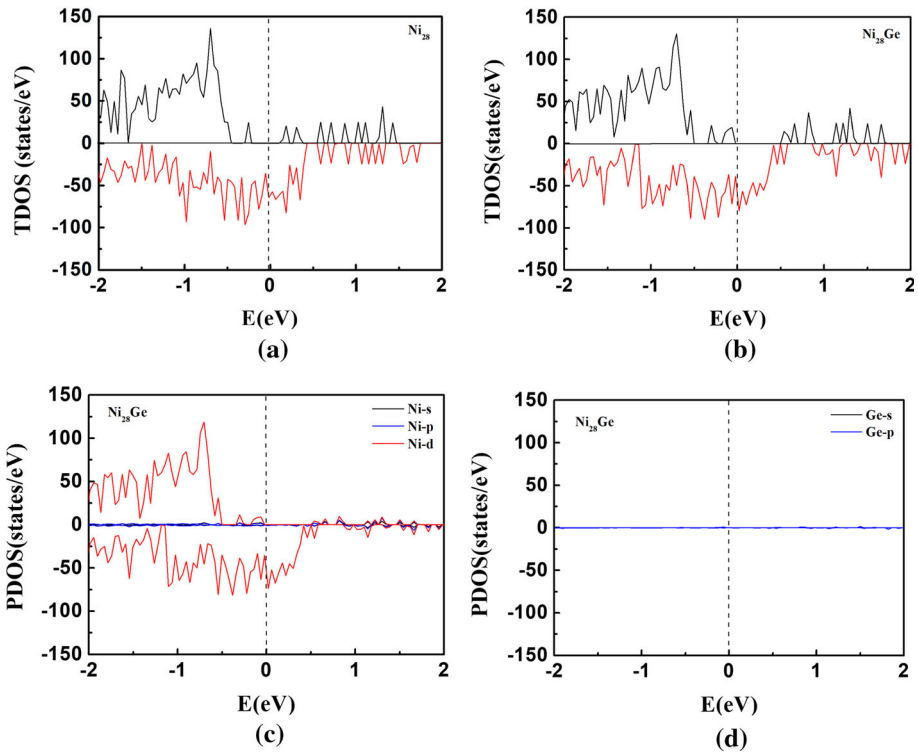

Fig. 5 The total (TDOS) and projected (PDOS) density of states for **a** Ni_{28} and **b**–**d** $Ni_{28}Gea$ clusters

double icosahedron and double icositetrahedron (with three parallel hexagonal rings), which exhibits high (C_{2v}) symmetry. This high symmetry makes the electronic state have a greater degree of degeneracy, resulting in high DOS. In addition, there is also charge transfer between the d orbit and s, p orbits of Ni (Fig. 5c), which leads to a reduction in the d-band width of $Ni_{28}Gea$ cluster and increasing the DOS, especially near the Fermi level. Finally exchange splitting induces a relative movement of the spin-up and spin-down band, which leads to different electron occupations in the spin-up and spin-down states, thus increasing the magnetic moment of $Ni_{28}Gea$ cluster. Next we have also plotted the total magnetic moment for the cationic and anionic clusters as shown in Fig. 4b, c, respectively. Similar to the corresponding neutral clusters, the total magnetic moment of $Ni_n^{+/-}$ is larger than that of $Ni_nGe^{+/-}$ except $Ni_{28}^{+/-}$ ($Ni_{28}Ge^{+/-}$). And the total magnetic moments of $Ni_{19}Ge^{+/-}$ and $Ni_{20}Ge^{-}$ are very close to $Ni_{19}^{+/-}$ and Ni_{20}^{-}. The results obtained by the present study help us choose magnetic materials.

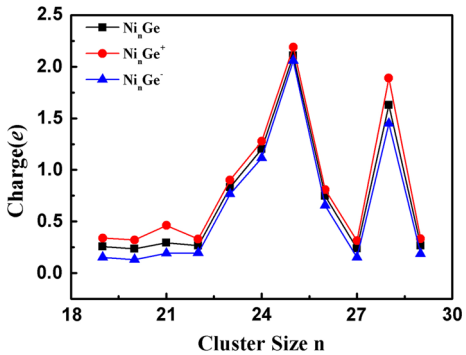

Fig. 6 Charge transfer (in units of *e*) from Ge atom to Ni_n (n = 19–29) clusters

Charge Transfer

The charge transfer between the Ge atom and Ni clusters for neutral and ionic Ni_nGea (n = 19–29) clusters are displayed in Fig. 6. Compared to the pure Ni_n clusters, the adsorption of Ge atom makes the electron cloud between the atoms lean toward the side of Ni_n clusters, and the electrons are transferred from the Ge atom to Ni_n clusters. In general, the electronegative of Ge(2.01) is more than

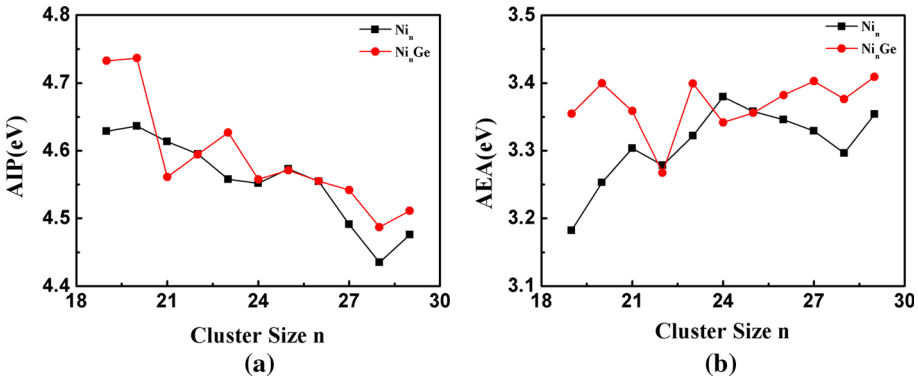

Fig. 7 **a** The adiabatic ionization potential (AIP) and **b** the adiabatic electron affinity (AEA) of Ni_n and Ni_nGea (n = 19–29) clusters

Ni(1.91). But Mulliken population analysis showed that, in this system, charge is always transferred from Ge to Ni, so Ge acts as an electron donor in Ni_nGe clusters. This mainly has two side reasons. On one hand, the whole Ni clusters have stronger electron withdrawing ability; on the other hand, the Ni atom has a large number of charges than Ge atom, so the transfer of electrons from Ge atom to Ni clusters. We find the amount of the charge transfer is less than $0.5e$ as a function of cluster size for Ni_nGea (n = 19–22, 27 and 29) clusters, and the cationic clusters is larger than that for neutral and anionic clusters. And the local maxima value has appeared at $Ni_{25}Gea$ cluster.

Ionization Potential and Electron Affinity

The adiabatic ionization potential (AIP) is an important character in understanding the electronic properties of clusters, and it can also account for the metallicity of the clusters. The calculated AIP for Ni_n and Ni_nGea (n = 19–29) clusters are shown in Fig. 7a. It can be seen from the plot that the AIP exhibits an oscillating behavior as the cluster size increases for Ni_n and Ni_nGea clusters. And the AIP is larger for Ni_nGea than that for Ni_n clusters except Ni_{21} ($Ni_{21}Gea$). And the AIP is very close to each other for n = 22, 24–26. As is well known, when the AIP gets smaller, the cluster will be more close to a metallic system; hence the metallicity is weakened with the addition of Ge atom. And the strongest metallicity is $Ni_{28}Gea$ cluster, which can be applied in the field of alloy materials.

The adiabatic electron affinity (AEA) for Ni_n and Ni_nGea (n = 19–29) clusters have been plotted in Fig. 7b as a function of cluster size. The clusters with greater AEA are more reactive. Similar to the trend of AIP, the AEA also exhibits an oscillating behavior as the cluster size increases for Ni_n and Ni_nGea clusters. The local maxima and minima of the AEA are Ni_{24} and Ni_{19} for Ni_n clusters, $Ni_{29}Gea$ and $Ni_{22}Gea$ for Ni_nGea clusters, respectively. And $Ni_{20}Gea$, $Ni_{23}Gea$, $Ni_{27}Gea$ and $Ni_{29}Gea$ clusters have the stronger ability to capture electrons.

Summary

The properties of the Ni_nGe (n = 19–29) clusters have been studied using the DFT-PBE calculations. In this work, we focused on analyzing a series of properties of the lowest-energy Ni-Ge alloy clusters including binding energy, embedding energy, magnetic property, charge transfer, ionization potential and electron affinity. The binding energies of Ni_nGe clusters are higher than the corresponding Ni_n clusters, and the curve of the binding energies is increasing monotonically as a function of cluster size. From the magnetic moment analyses, it is found that the addition of the Ge atom can decrease the magnetic moments of Ni_n clusters except Ni_{28} and $Ni_{28}^{+/-}$, but the Ge atom in all these clusters has negligible magnetic moments. On the other hand, the charge is transferred from Ge atom to Ni clusters. And the local maxima value has appeared at $Ni_{25}Ge$ cluster. Finally both the calculated ionization potential and electron affinity exhibit an oscillating behavior as the cluster size increases.

Acknowledgements This work is supported by the Natural Science Foundation of He'nan Department of Education (Grant Nos.: 15B150010; 18B430012 and 15A140032). This work is also supported by Xinxiang University Doctor Initial Research Program (Grant Nos.: 1366020018 and 1366020039) and Science and Technology Innovation Fund of Xinxiang University (Grant Nos.: 15ZP01 and 15ZB25). The computational resource is partly supported by the Performance Computing Center of Jilin University, China.

References

1. C. J. Feng and L. L. Cai (2014). *Comput. Theor. Chem.* **1042**, 57.
2. K. Dhaka, R. Trivedi, and D. Bandyopadhyay (2013). *J. Mol. Model.* **19**, 1473.
3. Z. W. Ma and B. X. Li (2015). *Comput. Theor. Chem.* **1068**, 88.
4. T. Mohri (2015). *J. Mater. Sci.* **50**, 7705.
5. J. Teeriniemi, J. Huisman, P. Taskinen, and K. Laasonen (2015). *J. Alloys Compd.* **652**, 371.
6. J. X. Zhu, P. Cheng, N. Wang, and S. P. Huang (2015). *Comput. Theor. Chem.* **1071**, 9.
7. N. S. Venkataramanan, R. Sahara, H. Mizuseki, and Y. Kawazoe (2010). *J. Phys. Chem. A* **114**, 5049.

8. J. A. Mary, A. Manikandan, L. J. Kennedy, M. Bououdina, R. Sundaram, and J. J. Vijaya (2014). *Trans. Nonferrous Met. Soc.* **24**, 1467.
9. B. R. Wang, H. Y. Han, and Z. Xie (2014). *J. Mol. Struct.* **1062**, 174.
10. C. M. Tang, M. Y. Liu, W. H. Zhu, and K. M. Deng (2011). *Comput. Theor. Chem.* **969**, 56.
11. N. Kapila, V. K. Jindal, and H. Sharma (2011). *Physica B* **406**, 4612.
12. A. Chikhaoui, K. Haddab, S. Bouarab, and A. Vega (2011). *J. Phys. Chem. A* **115**, 13997.
13. X. J. Deng, X. Y. Kong, X. L. Xu, H. G. Xu, and W. J. Zheng (2016). *Chin. J. Chem. Phys.* **29**, 123.
14. J. M. Goicoechea and J. E. McGrady (2015). *Dalton Trans.* **44**, 6755.
15. Z. El-Bayyari (2005). *J. Mol. Struct. (Theochem)* **716**, 165.
16. Z. Xie, Q. M. Ma, Y. Liu, and Y. C. Li (2005). *Phys. Lett. A* **342**, 459.
17. W. Song, W. C. Lu, Q. J. Zang, C. Z. Wang, and K. M. Ho (2012). *Int. J. Quantum Chem.* **112**, 1717.
18. W. Song, W. C. Lu, C. Z. Wang, and K. M. Ho (2011). *Comput. Theor. Chem.* **978**, 41.
19. G. Kresse and J. Hafner (1993). *Phys. Rev. B* **47**, 558.
20. G. Kresse and J. Furthmuller (1996). *Phys. Rev. B* **54**, 11169.
21. M. B. Abreu, A. C. Reber, and S. N. Khanna (2014). *J. Phys. Chem. Lett.* **5**, 3492.
22. D. Bandyopadhyay and P. Sen (2010). *J. Phys. Chem. A* **114**, 1835.
23. S. N. Khanna, B. Rao, and P. Jena (2002). *Phys. Rev. Lett.* **89**, 016803.
24. D. Bandyopadhyay, P. Kaur, and P. Sen (2010). *J. Phys. Chem. A* **114**, 12986.
25. R. Trivedi, K. Dhaka, and D. Bandyopadhyay (2014). *RSC Adv.* **4**, 64825.
26. D. Bandyopadhyay (2008). *J. Appl. Phys.* **104**, 084308.
27. M. Kumar, N. Bhattacharyya, and D. Bandyopadhyay (2012). *J. Mol. Model.* **18**, 405.
28. J. T. Lau, A. Föhlisch, M. Martins, R. Nietubyc, M. Reif, and W. Wurth (2002). *New J. Phys.* **4**, 98.